

1 **Diversity and composition of gut microbiome of cervical cancer patients by 16S**
2 **rRNA and whole-metagenome sequencing**

3 Greyson Biegert^{1*}, BS, Tatiana Karpinets^{2*}, PhD, Xiaogang Wu², PhD, Molly B. El
4 Alam¹, MPH, Travis T. Sims³, MD, MPH, Kyoko Yoshida-Court¹, PhD, Erica J. Lynn¹,
5 BS, Jingyan Yue¹, BS, Andrea Delgado Medrano¹, BS, Joseph Petrosino⁴, PhD,
6 Melissa P. Mezzari⁴, PhD, Nadim J. Ajami², PhD, Travis Solley¹, BS, Mustapha Ahmed-
7 Kaddar¹, BS, Lauren Elizabeth Colbert¹⁺, MD, MSCR, Ann H. Klopp¹⁺, MD, PhD

8 ¹Department of Radiation Oncology, The University of Texas MD Anderson Cancer
9 Center, Houston, TX, USA. ²Department of Genomic Medicine, The University of Texas
10 MD Anderson Cancer Center, Houston, TX, USA. ³Department of Gynecologic Oncology
11 and Reproductive Medicine, The University of Texas MD Anderson Cancer Center,
12 Houston, TX, USA. ⁴Department of Molecular Virology and Microbiology, Alkek Center for
13 Metagenomics and Microbiome Research, Baylor College of Medicine, Houston, TX,
14 USA.

15 * Authors Contributed Equally

16 +Shared corresponding authorship

17 Department of Radiation Oncology, Unit 1422, The University of Texas MD Anderson
18 Cancer Center, 1515 Holcombe Boulevard, Houston, TX 77030, USA (L.E. Colbert and
19 A.H. Klopp).

20 Telephone: 832-652-6033; fax: 713-745-2398; e-mail: lcolbert@mdanderson.org (L.E.
21 Colbert) and Telephone: 713-563-2444; fax: 713-745-2398; e-mail:
22 aklopp@mdanderson.org (A.H. Klopp).

Biegert et al 2020

23

24 **Running Title** (54 characters)

25 Comparison of 16S and WMS in the gut microbiome.

26

27 **Importance** (150 words)

28 The gut microbiome plays an important role in regulating human health and disease. 16S
29 rRNA gene sequencing (16S) and the whole-metagenome shotgun DNA sequencing
30 (WMS) are two approaches to describe the microbial community. 16S sequencing via any
31 amplicon sequencing-based method offers advantages over WMS in terms of precision
32 (specific gene targeting). Additionally, 16S has historically been less costly due to the
33 simplicity of library preparation and it does not require the same level read coverage as
34 WMS. In this study, we performed both sequencing methods on a single rectal swab
35 sample obtained from each cervical cancer patient prior to treatment. We showed that
36 these two methods provide comparable information for diversity, evenness, and richness
37 at higher taxonomic resolution, but are discrepant at a lower resolution. These
38 methodological findings provide valuable information for the design and interpretation of
39 future investigations of the role of the gut microbiome in cancer.

40

41 **Key Words**

42 16S rRNA gene sequencing, whole genome shotgun sequencing, gut microbiome,
43 cervical cancer

44

45 **Tweet** (optional: 256 words, please submit a Tweet that conveys the essential message
46 of your manuscript.) 16S may be sufficient for most initial studies of the gut microbiome
47 in cancer patients, but WMS may be required for analysis of lower level taxonomy.

48

49 **Conflicts of Interest:**

Biegert et al 2020

50 The authors report no conflicts of interest, financial or otherwise, related to the subject
51 matter of the article submitted.

52

53 **Research support:** This research was supported in part by the Radiological Society of
54 North America Resident/Fellow Award (to L.E.C.), the National Institutes of Health (NIH)
55 through MD Anderson's Cancer Center Support Grant P30CA016672, the Emerson
56 Collective and the National Institutes of Health T32 grant #5T32 CA101642-14 (T.T.S.).
57 This study was partially funded by The University of Texas MD Anderson Cancer Center
58 HPV-related Cancers Moonshot (L.E.C and A.K.).

59

60 **Abstract (250 words)**

61 Purpose Next generation sequencing has progressed rapidly, characterizing microbial
62 communities beyond culture-based or biochemical techniques. 16S ribosomal RNA gene
63 sequencing (16S) produces reliable taxonomic classifications and relative abundances,
64 while shotgun metagenome sequencing (WMS) allows higher taxonomic and functional
65 resolution at greater cost. The purpose of this study was to determine if 16S and WMS
66 provide congruent information for our patient population from paired fecal microbiome
67 samples.

68 Methods Patients with locally advanced cervical cancers were enrolled on a prospective,
69 observational clinical trial with a rectal swab sample collected prior to chemoradiation.
70 Bacterial DNA was extracted from each sample and divided in two parts for 16S or WMS
71 sequencing. We used measures of diversity richness and evenness as comparators of
72 16S and WMS sequencing. Relative abundances of the most common taxa were also

Biegert et al 2020

73 compared between both datasets. Both techniques were tested against baseline patient
74 demographics to assess associations identified with either or both methods.

75 **Results** Comparative indices were highly congruent between 16S and WMS. The most
76 abundant genera for 16S and WMS data did not overlap. Overlap was observed at the
77 Phylum level, as expected. However, relative abundances correlated poorly between the
78 two methodologies (all $p>0.05$). Hierarchical clustering of both sequencing analyses
79 identified overlapping enterotypes. Both approaches were in agreement with regard to
80 demographic variables.

81 **Conclusion** Diversity, evenness and richness are comparable when using 16S and WMS
82 techniques, however relative abundances of individual genera are not. Clinical
83 associations with diversity and evenness metrics were similarly identified with WMS or
84 16S.

85

86

87 **Introduction**

88 The gut microbiome is increasingly recognized as a critical determinant of health and
89 disease(1). The vast majority of microbiome analyses have utilized 16S rRNA gene
90 sequencing (16S) which uses variable regions of the 16S ribosomal RNA gene to assign
91 taxonomic classification and read abundance to calculate the relative frequency of the
92 organisms within a sample(2). 16S is a reliable method for identifying the relative
93 frequency of organisms but does not provide reliable functional information about the
94 genes encoded by these organisms(3). As a consequence, whole-metagenome
95 sequencing (WMS) data has been increasingly utilized with the goal of providing

Biegert et al 2020

96 functional information about the organisms present. WMS analyzes large swaths of
97 genomic information, which confers several advantages over 16S. Most notably, WMS
98 allows for an increased depth and specificity of sequenced species as well as insights
99 into gene abundance and metabolic capacity(4). Since WMS yields genomic information
100 beyond the 16S rRNA gene, it also confers a better assessment of the true diversity of
101 the sample. Thus, WMS can be used to provide species level resolution, as well as
102 differences in presence of microbial genes, articulated pathways and metabolic
103 functions(4). Yet, a limitation of shotgun sequence data is the large number of sequence
104 reads which must be mapped to databases, which requires significant expertise to
105 balance classification accuracy with discarded reads. Now, it is possible to analyze 16S
106 and WMS microbiome data side-by-side to investigate bacterial communities as well as
107 the abundance of associated genes and metabolic pathways(5–10). Still, the extent to
108 which these two sequencing methods correlate with one another is a critical assumption,
109 which should be explored thoroughly.

110

111 Few studies have had the opportunity to compare previously observed 16S gene
112 associations with data from WMS on the same cohort of patients(2). By subjecting the
113 same sample to both sequencing methods, we aim to investigate the reliability, validity
114 and reproducibility of these different approaches. To do so we utilized baseline gut
115 microbiome analysis from patients receiving standard chemoradiation therapy for cervical
116 cancer in order to examine and compare 16S microbiome associations with WMS data
117 on a variety of clinical variables. We deployed commonly used alpha diversity metrics
118 (Inverse Simpson Diversity, Shannon Diversity, Camargo Evenness, Pielou Evenness,

Biegert et al 2020

119 Observed Operational Taxonomic Units, and the Low Abundance Rarity Index) as well as
120 abundance measures, to draw comparisons between the two datasets. Additionally, we
121 submitted the datasets to unsupervised hierarchical clustering in order to assess if the
122 microbiome profiles associated together in a similar manner, as would be expected from
123 two datasets derived from a single sample source.

124

125 **Methods**

126 Study design and participants

127 We collected rectal swab samples from a cohort of 41 patients with newly diagnosed,
128 locally advanced cervical cancer undergoing treatment at The University of Texas MD
129 Anderson Cancer Center and Harris Health System Lyndon B. Johnson clinic. Patients
130 with previous pelvic radiation or treatment for cervical cancer were excluded. This study
131 was part of an IRB approved protocol (MDACC 2014-0543).

132 Patient population and treatment characteristics

133 Patients were enrolled in an IRB-approved (2014-0543) multi-institutional prospective
134 clinical trial at The University of Texas MD Anderson Cancer Center and the Harris Health
135 System, Lyndon B. Johnson General Hospital Oncology Clinic. Inclusion criteria were
136 newly diagnosed cervical cancer per the Federation of Gynecology and Obstetrics (FIGO)
137 2009 staging system, clinical stage IB1-IVA cancers, visible, exophytic tumor on
138 speculum examination with planned definitive treatment of intact cervical cancer with
139 external beam radiation therapy, cisplatin and brachytherapy. Patients with any previous
140 pelvic radiation therapy were excluded.

Biegert et al 2020

141 Patients underwent standard-of-care pretreatment evaluation for disease staging,
142 including tumor biopsy to confirm diagnosis; pelvic magnetic resonance imaging (MRI)
143 and positron emission tomography/computed tomography (PET/CT); and standard
144 laboratory evaluations, including a complete blood cell count, measurement of
145 electrolytes, and evaluation of renal and liver function. Patients received pelvic radiation
146 therapy to a total dose of 40–45 Gy delivered in daily fractions of 1.8 to 2 Gy over 4 to 5
147 weeks. Thereafter, patients received intracavitary brachytherapy with pulsed-dose-rate
148 or high-dose-rate treatments. Patients received cisplatin (40 mg/m² weekly) during
149 external beam radiation therapy according to standard institutional protocol. Patients
150 underwent repeat MRI at the completion of external beam radiation therapy or at the
151 time of brachytherapy, as indicated by the extent of disease. Patients with no residual
152 tumor on repeat MRI were considered to be exceptional responders while those with
153 residual MRI tumor volumes ≤20% and >20% of initial volumes after 4 to 5 weeks after
154 initiation of RT were considered to be standard and poor responders, respectively.

155 Sample collection and sequencing

156 Rectal swabs were collected in clinic at the time of rectal examination prior to treatment
157 using quick release matrix designed Isohelix swabs (Isohelix cat. SK-2S). We placed the
158 swabs in 400 µL of Lysis buffer and stored them at -80°C within 1 hour of sample
159 collection. One portion of each sample was sequenced using 16Sv4 rRNA sequencing
160 targeting the v4 region with primer 515F-806R(11), while another portion was sequenced
161 using WMS. 16S rRNA gene sequencing was performed through the Alkek Center for
162 Metagenomics and Microbiome Research (CMMR) at Baylor College of Medicine. 16S
163 rRNA gene sequencing methods were adapted from the methods developed for the Earth

Biegert et al 2020

164 Microbiome Project(11). Briefly, bacterial genomic DNA was extracted using MO BIO
165 PowerSoil DNA Isolation Kit (MO BIO Laboratories). The 16S rDNA V4 region was
166 amplified by PCR and sequenced on the MiSeq platform (Illumina) using the 2x250 bp
167 paired-end protocol yielding pair-end reads that overlap almost completely. The primers
168 used for amplification contain adapters for MiSeq sequencing and single-end barcodes
169 allowing pooling and direct sequencing of PCR products. Then gene sequences were
170 clustered into OTUs at a similarity cutoff value of 97% using the UPARSE algorithm(12).
171 To generate taxonomies, OTUs were mapped to an optimized version of the SILVA rRNA
172 database containing the 16S v4 region and then rarefied at 6989 reads. A custom script
173 was used to construct an OTU table from the output files generated as described above
174 for downstream analyses. Here, OTUs were selected as a basis for further analysis
175 because this method is currently the most common approach to 16s analysis in the clinical
176 research setting.

177 For WMS data, genomic bacterial DNA (gDNA) extraction methods optimized to maximize
178 the yield of bacterial DNA from specimens while keeping background amplification to a
179 minimum were employed(13, 14). Metagenomic shotgun sequencing was performed on
180 extracted total gDNA on Illumina sequencers using chemistries that yielded paired-end
181 reads. Sequencing reads were derived from raw BCL files which were retrieved from the
182 sequencer and called into fastqs by Casava v1.8.3 (Illumina). Then, paired-end reads
183 (fastq format) were filtered to remove Illumina PhiX sequences and trimmed for the
184 Illumina adapters by using bbduk in BBTools (version 38.34)(15). To remove host DNA
185 contamination, the trimmed reads were then mapped to a human reference sequence
186 database (hg38) by using Bowtie2 (version 2.3.5)(16). Taxonomic classification was

Biegert et al 2020

187 performed through MetaPhlAn2(17). Also based on Bowtie2, we mapped the cleaned
188 (unmapped to host genome) reads to a marker gene database
189 (mpa_v295_CHOCOPhIAn_201901, updated 11/11/2019) to get an individual relative
190 abundance table for each sample. Relative abundance tables for all samples were
191 merged and converted to a biom format (version 1.0)(18), which was then imported into
192 ATIMA (Agile Toolkit for Inclusive Microbial Analysis)(13) for statistical and diversity
193 analysis. Additionally, we obtained the functional annotation of the microbial community
194 by using HUMAnN2(6).

195 Alpha Diversity Indices

196 We then analyzed data from both WMS and 16S using several alpha diversity metrics
197 provided in the Microbiome R package(19) (R version 3.6.2), in order to assess the
198 richness, divergence and evenness of the microbial communities within each patient
199 sample. We calculated several index measures from observed OTU counts for 16S data
200 and WMS data collected from MetaPhlAn2 analysis independently. The Shannon
201 Diversity (SD)(20) and Inverse Simpson Diversity (ISD)(21) indexes provide a measure
202 of the total amount of species within a given sample. The Camargo(22) and Pielou(23)
203 Evenness indices are designed to calculate the proportionality of individual species within
204 a sample population. A high degree of evenness would imply that the abundances of all
205 individuals are roughly the same, or in equal proportions. Finally, the richness of the
206 datasets was calculated using Observed operational taxonomic unit (OTU) counts and
207 the Low Abundance Rarity (LAR) Index measures. The Observed OTUs index provides
208 a count based on the presence of at least one read for a given species within a sample.

Biegert et al 2020

209 The LAR index(19) instead characterizes the concentration of species which have low
210 abundance within the sample.

211

212 Comparative Statistical Analysis of 16S and WMS

213 We then paired each patient value from one dataset with its corresponding value for the
214 same patient in the other dataset. The amount of agreement between the two datasets,
215 in terms of alpha diversity measures, was then quantified using Spearman's rank
216 correlation coefficient (R or rho) with value of 1 indicating a perfect agreement, between
217 two sets of variables.

218 To assess the consistency in reporting microbial abundance between 16S and WMS, we
219 identified the most abundant taxa at the genus level for each sequencing method
220 independently. Then, we compiled a list of organisms on either of the lists. Thus, the next
221 set of comparisons were drawn using the total number of possible taxa identified by
222 taxonomic name at all phylogenetic levels (with the exception of species).

223 We also analyzed the datasets individually while considering patient demographic and
224 clinical characteristics. We analyzed six clinical variables to assess differences in
225 diversity, evenness, and richness between groups. Binary classifications were analyzed
226 using the independent t-test (Age, Smoking History, Histology) while multivariable
227 classifications were analyzed using One-Way ANOVA (Ethnicity, Node Level, FIGO
228 Stage). We also studied age and BMI as continuous variables in relation to Inverse
229 Simpson Diversity and Pielou evenness for both 16S and WMS datasets. Consensus
230 between the two datasets was defined as a $p \leq 0.1$ or >0.1 . All analyses were conducted
231 using R version 3.6.2 and Microsoft Excel (2016).

Biegert et al 2020

232 Hierarchical Clustering

233 To further explore the consistency of the two datasets, specifically the sample grouping
234 according to the putative taxa abundance profiles, we use unsupervised hierarchical
235 clustering of each OTU table by the cluster software with default settings(24). The data
236 used for clustering was limited by only using OTUs found in more than 14 samples. The
237 obtained heatmaps were visualized by the Java TreeView software(25).

238 Data Availability

239 Both 16S and WMS datasets will be available upon study completion and publication via
240 the database of Genotypes and Phenotypes (dbGaP). Similarly, proprietary code will be
241 available upon study completion and publication through GitHub.

242

243

244 **Results**

245 Taxonomic Composition and Abundance Using 16S and WMS

246 The number of putative taxa compiled in OTU tables was dramatically different between
247 the technologies, and included 984 OTUs in the 16S OTU table yet only 451 in the WMS
248 table. The WMS OTU table was not as sparse as the 16S table and had a different
249 abundance distribution frequency display, which was close to normal (Figure 1, panel 1).
250 The sparse 16S OTU table had significantly more rare low-abundance taxa; this feature
251 is evident from the frequency distribution (Figure 1, panel 2) and is well-characterized for
252 this type of dataset.

Biegert et al 2020

253 The top 10 most abundant phyla and genera found in 16S and WMS are shown in Figure
254 2. There was better consensus between 16S and WMS datasets on the phyla level than
255 on the genus level (Figure 2). The most abundant phyla identified in both 16S and WMS
256 were Bacteroides, Firmicutes, Proteobacteria, Actinobacteria and Fusobacteria.
257 Interestingly, Verrucomicrobia were found to be highly abundant only by WMS.
258 Tenericutes were ranked third most abundant by 16S but had low abundance according
259 to WMS. There was a significant mid-level association ($\rho=0.69$, $p=0.03$) between the
260 phyla abundances (Figure 2, panel 3). No significant associations between the
261 abundances were identified at other taxonomic levels.
262 None of the top abundant genera according to 16S were identified as the most abundant
263 genera according to WMS (Figure 2, panels 1 and 2). There was no overlap between the
264 top 10 most abundant genera in 16S and WMS. The top 10 genera in 16S or WMS are
265 listed in Table 1 with ranked relative abundances in each data set. Twelve genera were
266 present in either the top 10 of 16S or WMS and present at any rank level in the other data
267 set. Most genus level abundances correlated poorly between 16S and WMS ($\rho<0.15$).
268 The only genus, with relative abundance correlated well between the data sets, was
269 Peptoniphilus ($\rho=0.68$, $p<0.01$). The rest of the genera reported as the top 10 most
270 abundant in one dataset were not present in the other dataset, and thus no abundance
271 comparisons were made.
272 Consistent with the difference in frequency distribution of species abundances, the 16S
273 dataset included more putative species annotated at different taxonomic levels.
274 Furthermore, a high percentage of the taxa identified via 16S (58-67%) were not identified
275 by WMS, potentially as a result of using marker-gene classifiers. Conversely, most taxa

Biegert et al 2020

276 found in the WMS table were also identified by 16S (Figure 3). This percentage decreased
277 at low taxonomic levels.

278

279 **Diversity, Evenness, and Richness by 16S and WMS**

280 To further investigate the varied microbial compositions and abundances of taxa at most
281 phylogenetic levels, we next explored the effects of different general characteristics of
282 species diversity within the gut microbiomes. Surprisingly, we found that most indices of
283 diversity, evenness, and richness showed significant correlation between
284 16S and WMS datasets (Figure 4). All of the diversity and richness measures were tightly
285 correlated between 16S and WMS (ISD rho=0.89, p<0.01; SD rho=0.90, p=<0.01;
286 Observed OTUs rho=0.76, p<0.01; LAR rho=0.72, p<0.001) (Figure 4). Evenness indices
287 had a weaker correlation between 16S and WMS (Camargo rho=0.41, p<0.01; Pielou
288 rho=0.84, p<0.01), which is not surprising considering there was greater similarity in taxa
289 abundances in the WMS dataset than in the 16S dataset (Figure 1). Despite significant
290 differences in the rare OTUs, low abundance rarity indexes also significantly correlated
291 between the datasets. The slope of the regression line of the association was also
292 consistent with a significantly greater number of rare low abundance species in the 16S
293 dataset than in WMS.

294

295 **Association of Demographic Characteristics with diversity of microbiomes and specific**
296 **taxa**

297 In our next step, we investigated whether the differences and similarities considered
298 above affected biological conclusions drawn from each dataset. Namely, we explored

Biegert et al 2020

299 demographic variables (Supplementary Table 1) in association with gut microbiome
300 diversity and specific taxa using either the 16S or WMS dataset. When diversity,
301 evenness and richness indices were compared to baseline characteristics using both 16S
302 and WMS (Table 2), only age was associated with ISD in both WMS and 16S ($p<0.1$).
303 Age was associated with SD diversity ($p=0.04$), and Pielou evenness ($p=0.01$) using 16S,
304 but not WMS. Camargo evenness was associated with age only using WMS ($p=0.008$).
305 LAR richness was associated with BMI using WMS ($p=0.05$) but not 16S. Other baseline
306 demographic variables were not associated with diversity, evenness or richness using
307 any metric. Overall, there was consensus between methods (both $p\leq 0.1$ or >0.1) across
308 all demographics for ISD only. A positive correlation between age and gut diversity, and
309 between age and evenness was identified in both 16S (ISD; $\rho=0.37$, $p=0.02$. Pielou;
310 $\rho=0.39$, $p=0.01$) and WMS (ISD; $\rho=0.29$, $p=0.06$. Pielou; $\rho=0.28$, $p=0.08$) data
311 (Figure 5). Both datasets failed to find a difference between patient populations regarding
312 ethnicity, smoking status, tumor histology, nodal involvement, or FIGO Stage.
313 We further explored specific taxa associated with the age of cervical cancer patients using
314 Linear Discriminant Analysis (LDA) Effect Size (LEfSe). The clinical variable of age, was
315 classified in three different ways: over vs under 50 years of age, over vs under the median
316 age (49 years), and finally the patients were split into three sections where the 14
317 youngest and 14 oldest patients were compared against each other, with middle age
318 group omitted (SFig. 1). We applied the one-against-all strategy with a threshold of 3 on
319 the logarithmic LDA score for discriminative features and α of 0.05 for factorial Kruskal-
320 Wallis test among classes. Regardless of the classification method used, the taxa

Biegert et al 2020

321 identified as significantly enriched in older or younger patients was not consistent
322 between 16S and WMS datasets.

323

324 **Grouping of cervical cancer patients in terms of putative species abundances**

325 Unsupervised hierarchical clustering of samples based on the species abundances in
326 WMS and 16S (Figure 6) and OTU tables revealed 2 broad groups of patients in each
327 hierarchy with significant overlap among patients comprising each group (Fisher's Exact
328 Test p-value is 0.004) . Despite the significant differences in the number of genera
329 identified by 16S and WMS, the hierarchical clustering of OTUs was consistent between
330 datasets and revealed a set of OTUs enriched with *Prevotella*, *Peptoniphilus*, and
331 *Porphyromonas*. These genera were more abundant in both 16S and WMS Cluster 1,
332 but less abundant in 16S and WMS Cluster 2. Most notably, the grouping of patients in
333 Cluster 1 and 2 was associated with the BMI index of the patients (Fisher's Exact Test
334 p-value is 0.002 for WMS and 0.06 for 16S). There were significantly more patients with
335 BMI<median (28.63) in Cluster 1 (WMS and 16S) than in Cluster 2 (both datasets).
336 There were 20 patients in the 16S Cluster 1 and 24 patients in the WMS Cluster 1.
337 Thirteen of which were in common between those clusters, and they were grouped
338 close to one another. Indicating a greater degree of similarity in terms of their OTU
339 abundance profiles.

340

341 **Discussion**

342 This study is limited by our analytic pipelines and available samples, but the results
343 suggest that 16S with OTU clustering provides a similar description of sample diversity

Biegert et al 2020

344 and composition for gut microbiomes of cervical cancer patients versus WMS. This finding
345 is important, as it allows researchers to analyze a larger number of samples using 16S at
346 a fraction of the cost of WMS. Camargo evenness and skewness were the least correlated
347 indices between the two methodologies, which suggests that the sequencing methods
348 differ in terms of the proportionality of individual bacterial taxa. This might be improved
349 using a 16S analysis pipeline that uses amplicon sequence variants, such as QIIME2, to
350 retain more reads. The Camargo index has low sensitivity for variation in species diversity
351 for sample sizes <3000, while the Pielou index is a sensitive assessment index for smaller
352 sample sizes (<1000). Thus, the Pielou evenness index is more appropriate in terms of
353 this sample size, and correlates well between the two datasets(20). With regards to rare
354 taxa (LAR), WMS provides more noise in a dataset by identifying individual genes, which
355 may be linked to unidentified bacterial species. 16S combined with OTU clustering can at
356 best provide information at the genus level with a high degree of confidence and relies on
357 97% similarity clustering at the OTU level. This difference is to be expected, and could be
358 exploited in specific analyses, such as searching for previously identified species or
359 particular gene functions. It is reassuring that there was significant consensus between
360 the methodologies on the higher order levels. Much of the focus in next generation
361 sequencing analysis is placed on the smallest taxonomic level available (i.e. the genus
362 or species level), but higher order taxa also provide valuable information.

363 Previous work has also posited a sizable amount of agreement between 16S and
364 WMS sequencing techniques at higher orders of taxa(2), consistent with these results.
365 16S and WMS have a significant degree of correlation; however, most of those studies
366 utilize data derived from samples collected in similar but not identical contexts. This

Biegert et al 2020

367 project provides a unique opportunity in that both 16S and WMS sequencing datasets
368 were derived from a single sample collected from each patient and then bacterial DNA
369 was extracted for both methods. Using this high-quality information, we investigated the
370 correlation of these two datasets in terms of microbial composition abundance and alpha
371 diversity, to precisely determine how well these sequencing methods corroborated. Since
372 the two datasets are derived from the same samples, association with the clinical
373 variables should also result in the same conclusion regardless of the sequencing method
374 used, which was again confirmed. Age is perhaps the variable most strongly associated
375 with microbiome diversity, which was confirmed in both datasets in our study. It is also
376 important to note, hierarchical clustering analysis showed 9 (69%) out of 13 patients in
377 Cluster1 were white, while only 8 (31%) of the 28 patients in the rest of the cohort were
378 white. In addition, 12 (92%) out of the 13 patients in Cluster1 had a disease stage of 1 or
379 2, compared to 19 (68%) out of the 28 patients in the rest of the cohort.

380 An important limitation of the study that we focus solely on taxonomic
381 characteristics of the gut community. The major advantage of WMS is that it provides an
382 opportunity to assay functional diversity of the microbiome, a capability severely lacking
383 in 16S data. Tools such as PICRUSt(26) can infer metabolic profiles from 16S data, but
384 they cannot truly assemble functional pathways. Yet, the most fundamental drawback of
385 this study is due to the limitations of analytic pipelines used in each approach and the
386 databases available for both 16S and WMS data. Tools for analyzing 16s have been
387 developed and successfully deployed far longer than WMS analysis software, while the
388 WMS analysis pipelines and databases are continually being developed and shared. The
389 differences in alignment techniques and databases would account for a lot of the variation

Biegert et al 2020

390 in taxa names herein. For example, by calculating OTUs we recapitulated a popular
391 method of alignment used in this field, but in doing so the data has been collapsed at the
392 cost of potential diversity information. Additionally, tools used for metagenomic analysis
393 vary based on techniques used such as distance metrics and clustering approaches(15).
394 Here, we used OTU clustering at 97% similarity using previously described methodology
395 from the Human Microbiome Project(13), but this data could be re-analyzed using QIIME2
396 and amplicon sequence variant (ASV) calling(27) and result in variations in ASV vs. OTU
397 assignment that could affect the analysis. Amplicon sequence variant calling with DADA2
398 denoising(28) may be a preferable system for WMS comparisons as the pipeline is more
399 similar to how WMS reads are treated. Another important consideration is that the
400 MetaPhlAn2 tool inherent in the Humann2 pipeline uses a relatively small fraction of the
401 data generated, whereas another non-marker gene based identifier such as QIIME2,
402 Kraken 2(29) or the mothur software(30) will generate a larger and more varied, spread
403 of results. Still, MetaPhlAn2 outperformed IGGsearch(31) which was also deployed on
404 our WMS dataset, and it remains the most popular marker-gene based tool in the
405 metagenome field.

406 Another limitation to address, for this work and many others, is establishing a
407 confident rarefaction cut off for analysis. Usually this cut off value would be validated by
408 utilizing a mock microbial community dataset to be analyzed alongside experimental data.
409 Here, we were unable to acquire complete mock communities as such information is
410 privileged and difficult to attain. However, the cut off value we used was selected because
411 it was consistently stringent across both 16S and WMS datasets while retaining as much
412 information as possible.

Biegert et al 2020

413 All this is to say, variations in approaches to metagenome assembly pipelines
414 similarly could affect taxonomic assignment in 16S and WMS data. It is possible that a
415 particular sequence relevant to both datasets would be classified differently during
416 preprocessing, highlighting the necessity of universal reference databases and
417 sequencing alignment tools and protocol consensus.

418 Given this variability in sequencing and data processing pipelines, the use of
419 multiple techniques across different types of sequencing data is an excellent way to
420 confirm consistency in conclusions. However, limited resources (e.g. material from clinical
421 samples, bioinformatics support, time and finances) hamper the ability for this expansive
422 and in-depth microbiome profiling for all studies. Although WMS has been demonstrated
423 to confer significant advantages over 16S, this work suggests there is very little additional
424 taxonomic information identified from WMS that was not identified in 16S data. This can
425 vary depending on the context of analysis, for example method of sample collection (i.e.,
426 whole stool vs swabs) and determining the functional components of the microbiome in
427 question.(26, 32) It is even possible that extracting DNA from the same sample at two
428 different times, instead of splitting a single extraction as was done here, may yield slightly
429 different results. In our work, alpha diversity assessments such as overall diversity,
430 evenness and richness can provide meaningful, and more important, comparable
431 information (Figure 1) when obtained with either 16S or WMS. Furthermore, the two
432 datasets provided a high degree of consensus when these indices were subjected to
433 statistical analysis. This suggests that for studies where overall microbiome diversity,
434 richness and evenness are the goals of an analysis, 16S is more than sufficient to provide
435 this information. For basic taxonomic descriptions, there was a meaningful agreement on

Biegert et al 2020

436 the phyla and higher taxa levels, suggesting that 16S is also sufficient in this setting for
437 hypothesis-generating data. Nonetheless, these two datasets did provide some
438 differences in taxonomic assignment, particularly on the genus level, and relative
439 abundances of individual taxonomies. This suggests that for studies where a broader
440 repertoire of potential species are needed, both techniques may be necessary.

441 In all, this evidence suggests that using 16S alone may be sufficient in the clinical
442 cancer research setting, where available patient material, time and money can be scarce.
443 Based on these findings, we suggest 16S for the gut microbiome of cancer patients for
444 initial diversity, richness and evenness metrics along with higher level taxonomic
445 classification. WMS can provide a large swath of detailed microbial information, albeit
446 with less sensitivity than 16S, and may be ideal when additional information on genus
447 and species level identification is needed or to confirm conclusions drawn from 16S data.

448

449 **References**

450 1. Lynch SV, Pedersen O. 2016. The Human Intestinal Microbiome in Health and Disease. N
451 Engl J Med 375:2369–2379.

452 2. Vogtmann E, Hua X, Zeller G, Sunagawa S, Voigt AY, Hercog R, Goedert JJ, Shi J, Bork
453 P, Sinha R. 2016. Colorectal Cancer and the Human Gut Microbiome: Reproducibility with
454 Whole-Genome Shotgun Sequencing. PloS One 11:e0155362.

455 3. Laudadio I, Fulci V, Palone F, Stronati L, Cucchiara S, Carissimi C. 2018. Quantitative
456 Assessment of Shotgun Metagenomics and 16S rDNA Amplicon Sequencing in the Study
457 of Human Gut Microbiome. Omics J Integr Biol 22:248–254.

Biegert et al 2020

458 4. Salipante SJ, SenGupta DJ, Cummings LA, Land TA, Hoogestraat DR, Cookson BT. 2015.
459 Application of whole-genome sequencing for bacterial strain typing in molecular
460 epidemiology. *J Clin Microbiol* 53:1072–1079.

461 5. Zolfo M, Asnicar F, Manghi P, Pasolli E, Tett A, Segata N. 2018. Profiling microbial strains
462 in urban environments using metagenomic sequencing data. *Biol Direct* 13:9.

463 6. Franzosa EA, McIver LJ, Rahnavard G, Thompson LR, Schirmer M, Weingart G, Lipson
464 KS, Knight R, Caporaso JG, Segata N, Huttenhower C. 2018. Species-level functional
465 profiling of metagenomes and metatranscriptomes. *Nat Methods* 15:962–968.

466 7. Pasolli E, Asnicar F, Manara S, Zolfo M, Karcher N, Armanini F, Beghini F, Manghi P, Tett
467 A, Ghensi P, Collado MC, Rice BL, DuLong C, Morgan XC, Golden CD, Quince C,
468 Huttenhower C, Segata N. 2019. Extensive Unexplored Human Microbiome Diversity
469 Revealed by Over 150,000 Genomes from Metagenomes Spanning Age, Geography, and
470 Lifestyle. *Cell* 176:649–662.e20.

471 8. Vatanen T, Plichta DR, Somani J, Münch PC, Arthur TD, Hall AB, Rudolf S, Oakeley EJ,
472 Ke X, Young RA, Haiser HJ, Kolde R, Yassour M, Luopajarvi K, Siljander H, Virtanen SM,
473 Ilonen J, Uibo R, Tillmann V, Mokurov S, Dorshakova N, Porter JA, McHardy AC,
474 Lähdesmäki H, Vlamakis H, Huttenhower C, Knip M, Xavier RJ. 2019. Genomic variation
475 and strain-specific functional adaptation in the human gut microbiome during early life. *Nat
476 Microbiol* 4:470–479.

477 9. Franzosa EA, Sirota-Madi A, Avila-Pacheco J, Fornelos N, Haiser HJ, Reinker S, Vatanen
478 T, Hall AB, Mallick H, McIver LJ, Sauk JS, Wilson RG, Stevens BW, Scott JM, Pierce K,
479 Deik AA, Bullock K, Imhann F, Porter JA, Zhernakova A, Fu J, Weersma RK, Wijmenga C,
480 Clish CB, Vlamakis H, Huttenhower C, Xavier RJ. 2019. Gut microbiome structure and
481 metabolic activity in inflammatory bowel disease. *Nat Microbiol* 4:293–305.

482 10. Vila AV, Imhann F, Collij V, Jankipersadsing SA, Gurry T, Mujagic Z, Kurilshikov A, Bonder
483 MJ, Jiang X, Tigchelaar EF, Dekens J, Peters V, Voskuil MD, Visschedijk MC, Dullemen

Biegert et al 2020

484 HM van, Keszthelyi D, Swertz MA, Franke L, Alberts R, Festen EAM, Dijkstra G, Masclee
485 AAM, Hofker MH, Xavier RJ, Alm EJ, Fu J, Wijmenga C, Jonkers DMAE, Zhernakova A,
486 Weersma RK. 2018. Gut microbiota composition and functional changes in inflammatory
487 bowel disease and irritable bowel syndrome. *Sci Transl Med* 10.

488 11. Thompson LR, Sanders JG, McDonald D, Amir A, Ladau J, Locey KJ, Prill RJ, Tripathi A,
489 Gibbons SM, Ackermann G, Navas-Molina JA, Janssen S, Kopylova E, Vázquez-Baeza Y,
490 González A, Morton JT, Mirarab S, Zech Xu Z, Jiang L, Haroon MF, Kanbar J, Zhu Q, Jin
491 Song S, Kosciolek T, Bokulich NA, Lefler J, Brislawn CJ, Humphrey G, Owens SM,
492 Hampton-Marcell J, Berg-Lyons D, McKenzie V, Fierer N, Fuhrman JA, Clauset A, Stevens
493 RL, Shade A, Pollard KS, Goodwin KD, Jansson JK, Gilbert JA, Knight R. 2017. A
494 communal catalogue reveals Earth's multiscale microbial diversity. 7681. *Nature* 551:457–
495 463.

496 12. Edgar RC. 2013. UPARSE: highly accurate OTU sequences from microbial amplicon
497 reads. 10. *Nat Methods* 10:996–998.

498 13. The Human Microbiome Project Consortium. 2012. A framework for human microbiome
499 research. *Nature* 486:215–221.

500 14. Huttenhower C, Gevers D, Knight R, Abubucker S, Badger JH, Chinwalla AT, Creasy HH,
501 Earl AM, FitzGerald MG, Fulton RS, Giglio MG, Hallsworth-Pepin K, Lobos EA, Madupu R,
502 Magrini V, Martin JC, Mitreva M, Muzny DM, Sodergren EJ, Versalovic J, Wollam AM,
503 Worley KC, Wortman JR, Young SK, Zeng Q, Aagaard KM, Abolude OO, Allen-Vercoe E,
504 Alm EJ, Alvarado L, Andersen GL, Anderson S, Appelbaum E, Arachchi HM, Armitage G,
505 Arze CA, Ayvaz T, Baker CC, Begg L, Belachew T, Bhonagiri V, Bihan M, Blaser MJ,
506 Bloom T, Bonazzi V, Paul Brooks J, Buck GA, Buhay CJ, Busam DA, Campbell JL, Canon
507 SR, Cantarel BL, Chain PSG, Chen I-MA, Chen L, Chhibba S, Chu K, Ciulla DM, Clemente
508 JC, Clifton SW, Conlan S, Crabtree J, Cutting MA, Davidovics NJ, Davis CC, DeSantis TZ,
509 Deal C, Delehaunty KD, Dewhurst FE, Deych E, Ding Y, Dooling DJ, Dugan SP, Michael

Biegert et al 2020

510 Dunne W, Scott Durkin A, Edgar RC, Erlich RL, Farmer CN, Farrell RM, Faust K,
511 Feldgarden M, Felix VM, Fisher S, Fodor AA, Forney LJ, Foster L, Di Francesco V,
512 Friedman J, Friedrich DC, Fronick CC, Fulton LL, Gao H, Garcia N, Giannoukos G, Giblin
513 C, Giovanni MY, Goldberg JM, Goll J, Gonzalez A, Griggs A, Gujja S, Kinder Haake S,
514 Haas BJ, Hamilton HA, Harris EL, Hepburn TA, Herter B, Hoffmann DE, Holder ME,
515 Howarth C, Huang KH, Huse SM, Izard J, Jansson JK, Jiang H, Jordan C, Joshi V,
516 Katancik JA, Keitel WA, Kelley ST, Kells C, King NB, Knights D, Kong HH, Koren O, Koren
517 S, Kota KC, Kovar CL, Kyrides NC, La Rosa PS, Lee SL, Lemon KP, Lennon N, Lewis
518 CM, Lewis L, Ley RE, Li K, Liolios K, Liu B, Liu Y, Lo C-C, Lozupone CA, Dwayne
519 Lunsford R, Madden T, Mahurkar AA, Mannon PJ, Mardis ER, Markowitz VM, Mavromatis
520 K, McCollum JM, McDonald D, McEwen J, McGuire AL, McInnes P, Mehta T,
521 Mihindukulasuriya KA, Miller JR, Minx PJ, Newsham I, Nusbaum C, O'Laughlin M, Orvis J,
522 Pagani I, Palaniappan K, Patel SM, Pearson M, Peterson J, Podar M, Pohl C, Pollard KS,
523 Pop M, Priest ME, Proctor LM, Qin X, Raes J, Ravel J, Reid JG, Rho M, Rhodes R, Riehle
524 KP, Rivera MC, Rodriguez-Mueller B, Rogers Y-H, Ross MC, Russ C, Sanka RK, Sankar
525 P, Fah Sathirapongsasuti J, Schloss JA, Schloss PD, Schmidt TM, Scholz M, Schriml L,
526 Schubert AM, Segata N, Segre JA, Shannon WD, Sharp RR, Sharpton TJ, Shenoy N,
527 Sheth NU, Simone GA, Singh I, Smillie CS, Sobel JD, Sommer DD, Spicer P, Sutton GG,
528 Sykes SM, Tabbaa DG, Thiagarajan M, Tomlinson CM, Torralba M, Treangen TJ, Truty
529 RM, Vishnivetskaya TA, Walker J, Wang L, Wang Z, Ward DV, Warren W, Watson MA,
530 Wellington C, Wetterstrand KA, White JR, Wilczek-Boney K, Wu Y, Wylie KM, Wylie T,
531 Yandava C, Ye L, Ye Y, Yooseph S, Youmans BP, Zhang L, Zhou Y, Zhu Y, Zoloth L,
532 Zucker JD, Birren BW, Gibbs RA, Highlander SK, Methé BA, Nelson KE, Petrosino JF,
533 Weinstock GM, Wilson RK, White O, The Human Microbiome Project Consortium. 2012.
534 Structure, function and diversity of the healthy human microbiome. 7402. Nature 486:207–
535 214.

Biegert et al 2020

536 15. Bushnell B, Rood J, Singer E. 2017. BBMerge – Accurate paired shotgun read merging via
537 overlap. *PLOS ONE* 12:e0185056.

538 16. Langmead B, Salzberg SL. 2012. Fast gapped-read alignment with Bowtie 2. *Nat Methods*
539 9:357–359.

540 17. McDonald D, Clemente JC, Kuczynski J, Rideout JR, Stombaugh J, Wendel D, Wilke A,
541 Huse S, Hufnagle J, Meyer F, Knight R, Caporaso JG. 2012. The Biological Observation
542 Matrix (BIOM) format or: how I learned to stop worrying and love the ome-ome.
543 *GigaScience* 1.

544 18. Truong DT, Franzosa EA, Tickle TL, Scholz M, Weingart G, Pasolli E, Tett A, Huttenhower
545 C, Segata N. 2015. MetaPhlAn2 for enhanced metagenomic taxonomic profiling. *Nat*
546 *Methods* 12:902–903.

547 19. Lahti L, Shetty S, Obenchain V, Turaga N. Tools for microbiome analysis in R. Version
548 1.9.19.

549 20. Mouillot D, Leprêtre A. 1999. A comparison of species diversity estimators. *Popul Ecol*
550 41:203–215.

551 21. Hill MO. 1973. Diversity and Evenness: A Unifying Notation and Its Consequences.
552 *Ecology* 54:427–432.

553 22. Camargo JA. 1995. On Measuring Species Evenness and Other Associated Parameters of
554 Community Structure. *Oikos* 74:538–542.

555 23. Pielou EC. 1966. The measurement of diversity in different types of biological collections. *J*
556 *Theor Biol* 13:131–144.

557 24. Bronstein M, Deutsch M. 1991. Early diagnosis of proximal femoral deficiency. *Gynecol*
558 *Obstet Invest* 34:246–248.

559 25. Saldanha AJ. 2004. Java Treeview--extensible visualization of microarray data. *Bioinforma*
560 *Oxf Engl* 20:3246–3248.

561 26. Langille MGI, Zaneveld J, Caporaso JG, McDonald D, Knights D, Reyes JA, Clemente JC,

Biegert et al 2020

562 Burkepile DE, Vega Thurber RL, Knight R, Beiko RG, Huttenhower C. 2013. Predictive
563 functional profiling of microbial communities using 16S rRNA marker gene sequences. *Nat*
564 *Biotechnol* 31:814–821.

565 27. Bolyen E, Rideout JR, Dillon MR, Bokulich NA, Abnet CC, Al-Ghalith GA, Alexander H,
566 Alm EJ, Arumugam M, Asnicar F, Bai Y, Bisanz JE, Bittinger K, Brejnrod A, Brislawn CJ,
567 Brown CT, Callahan BJ, Caraballo-Rodríguez AM, Chase J, Cope EK, Da Silva R, Diener
568 C, Dorrestein PC, Douglas GM, Durall DM, Duvallet C, Edwardson CF, Ernst M, Estaki M,
569 Fouquier J, Gauglitz JM, Gibbons SM, Gibson DL, Gonzalez A, Gorlick K, Guo J, Hillmann
570 B, Holmes S, Holste H, Huttenhower C, Huttley GA, Janssen S, Jarmusch AK, Jiang L,
571 Kaehler BD, Kang KB, Keefe CR, Keim P, Kelley ST, Knights D, Koester I, Kosciolek T,
572 Kreps J, Langille MGI, Lee J, Ley R, Liu Y-X, Loftfield E, Lozupone C, Maher M, Marotz C,
573 Martin BD, McDonald D, McIver LJ, Melnik AV, Metcalf JL, Morgan SC, Morton JT, Naimey
574 AT, Navas-Molina JA, Nothias LF, Orchanian SB, Pearson T, Peoples SL, Petras D,
575 Preuss ML, Pruesse E, Rasmussen LB, Rivers A, Robeson MS, Rosenthal P, Segata N,
576 Shaffer M, Shiffer A, Sinha R, Song SJ, Spear JR, Swafford AD, Thompson LR, Torres PJ,
577 Trinh P, Tripathi A, Turnbaugh PJ, Ul-Hasan S, van der Hooft JJJ, Vargas F, Vázquez-
578 Baeza Y, Vogtmann E, von Hippel M, Walters W, Wan Y, Wang M, Warren J, Weber KC,
579 Williamson CHD, Willis AD, Xu ZZ, Zaneveld JR, Zhang Y, Zhu Q, Knight R, Caporaso JG.
580 2019. Reproducible, interactive, scalable and extensible microbiome data science using
581 QIIME 2. *Nat Biotechnol* 37:852–857.

582 28. Callahan BJ, McMurdie PJ, Rosen MJ, Han AW, Johnson AJA, Holmes SP. 2016. DADA2:
583 High-resolution sample inference from Illumina amplicon data. *7. Nat Methods* 13:581–
584 583.

585 29. Wood DE, Salzberg SL. 2014. Kraken: ultrafast metagenomic sequence classification
586 using exact alignments. *Genome Biol* 15:R46.

587 30. Schloss PD, Westcott SL, Ryabin T, Hall JR, Hartmann M, Hollister EB, Lesniewski RA,

Biegert et al 2020

588 Oakley BB, Parks DH, Robinson CJ, Sahl JW, Stres B, Thallinger GG, Horn DJV, Weber
589 CF. 2009. Introducing mothur: Open-Source, Platform-Independent, Community-Supported
590 Software for Describing and Comparing Microbial Communities. *Appl Environ Microbiol*
591 75:7537–7541.
592 31. New insights from uncultivated genomes of the global human gut microbiome | *Nature*.
593 32. Ranjan R, Rani A, Metwally A, McGee HS, Perkins DL. 2016. Analysis of the microbiome:
594 Advantages of whole genome shotgun versus 16S amplicon sequencing. *Biochem Biophys
595 Res Commun* 469:967–977.

596 **Tables**

597 **Table 1. Comparisons of Top Ranked WMS and 16S Genera.**

598 The top ten most abundant Genera identified in WMS or 16S (identified with *) are
599 shown next to their counterpart and the associated rank. Genera present in both lists
600 were correlated in terms of abundance using Spearman R. Resulting p values are
601 shown as not significant (ns), less than 0.1 (bold), or less than 0.05 (red). Genera
602 present in one dataset, but not the other (-) could not be correlated.

<u>Genus Name</u>	<u>WMS Rank</u>	<u>16S RNA Rank</u>	<u>Spearman R</u>	<u>p Value</u>
Bacteroides	1*	12	0.29	0.0639
Prevotella	2*	70	0.21	ns
Parabacteroides	3*	88	0.09	ns
Porphyromonas	4*	126	-0.1	ns
Akkermansia	5*	129	0.18	ns
Alistipes	6*	13	-0.27	0.0828
Faecalibacterium	7*	-	-	-
Campylobacter	8*	115	0.05	ns
Peptoniphilus	9*	56	0.68	1.14E-06

Biegert et al 2020

Oscillibacter	10*	34	0.12	ns
Mycoplasma	58	9*	0.24	ns
Coprobacter	73	7*	0.22	ns
Jonquetella	119	5*	-0.18	ns
Nocardioides	-	1*	-	-
Lachnoanaerobaculum	-	2*	-	-
Clostridium sensu stricto 1	-	3*	-	-
Ruminococcaceae UCG_014	-	4*	-	-
Selenomonas_4	-	6*	-	-
Eubacterium coprostanoligenes group	-	8*	-	-
Christensenellaceae R_7_group	-	10*	-	-

603

604 **Table 2. Correlation between WMS and 16sRNA in terms of Diversity, Evenness,**
605 **and Richness.**

606 In this table, patient demographics and clinical assessments were collected and used as
607 classification criteria to investigate differences between these characteristics in terms of
608 alpha diversity measurements discussed earlier. Both datasets were analyzed using
609 either a parametric t-test [Smoking History (Yes/No), Histology
610 (Adenocarcinoma/Squamous Cell Carcinoma)], linear regression [Age and BMI], or
611 One-Way ANOVA [Ethnicity (White, Black, Hispanic, Other), Node Level (Common
612 Iliac/External Iliac/Internal Iliac/None/Para-Aortic), FIGO Stage (IA1, IB1, IB2, IBI, IIA,
613 IIB, IIIB, IVA)]. The resulting p value measures are indicated on the table as being either
614 non-significant (ns), less than 0.1 (black) or less than 0.05 (red). Consensus between
615 both methods, whole-metagenome sequencing and 16sRNA sequencing, indicates the
616 validity of using either method for exploring that clinical variable.

617

618

619

620

621

622

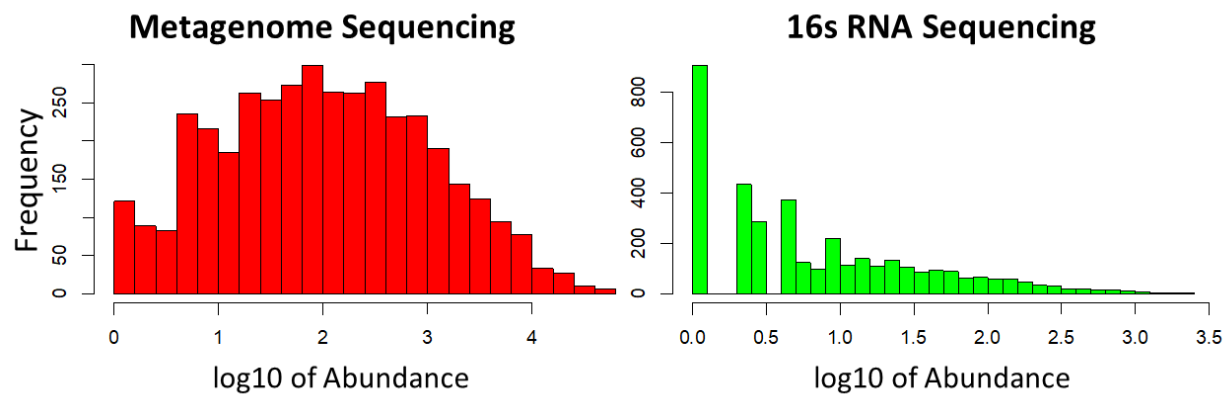
Clinical Variable	Diversity				Evenness				Richness			
	Inverse Simpson		Shannon		Camargo		Pielou		Observed OTUs		LAR	
	WMS	16sRNA	WMS	16sRNA	WMS	16sRNA	WMS	16sRNA	WMS	16sRNA	WMS	16sRNA
Age	0.0631	0.0166	ns	0.0396	0.0077	ns	ns	0.0111	ns	ns	ns	ns
Ethnicity (W,B,H,O)	ns	ns	ns	ns	ns	ns	ns	ns	ns	ns	ns	ns
Smoking History (Y/N)	ns	ns	ns	ns	ns	ns	ns	ns	ns	ns	ns	ns
Histology (Adeno/Squam)	ns	ns	ns	ns	ns	ns	ns	ns	ns	ns	ns	ns
Node level	ns	ns	ns	ns	ns	ns	ns	ns	0.0748	ns	ns	ns
FIGO Stage	ns	ns	ns	ns	ns	ns	ns	ns	ns	ns	ns	ns
BMI	ns	ns	ns	ns	ns	ns	ns	ns	ns	ns	0.0468	ns

623

624

625

626 **Figures**

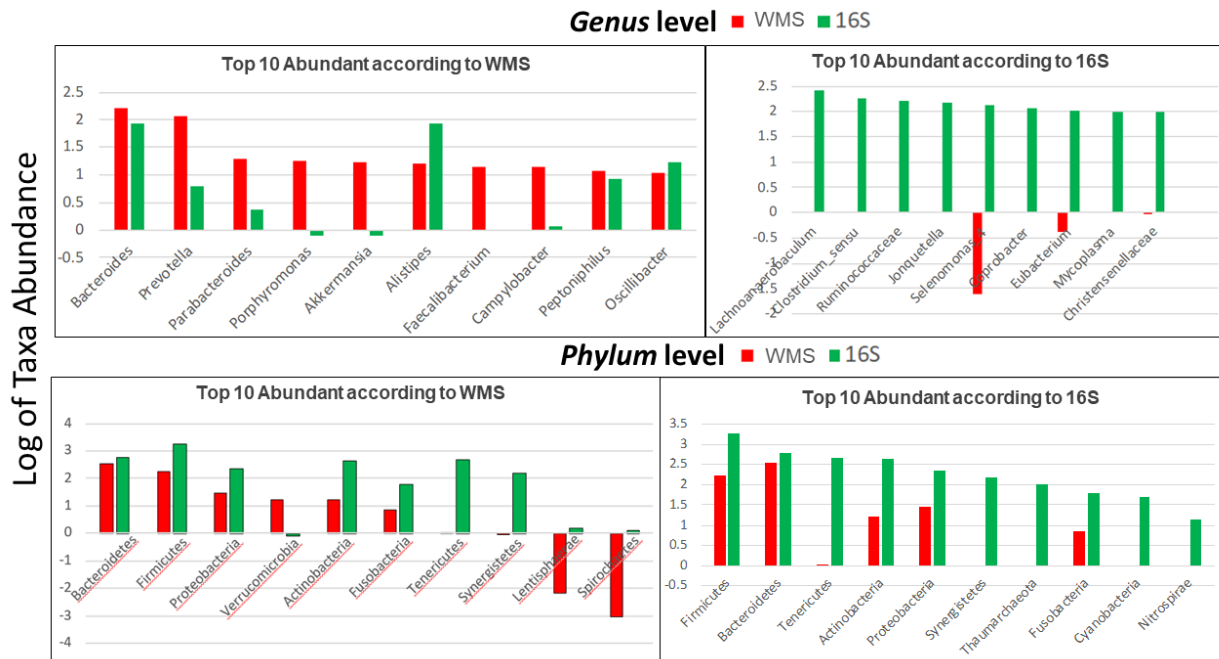


627

628 **Figure 1. Different distribution of putative taxa species abundance in WMS and in**
629 **16S OTU tables.**

630 To display differences in abundances in terms of OTU frequencies, OTU counts were
631 log transformed and presented here as histograms. WMS (red) OTU identifiers
632 displayed reduced overall frequency compared to 16S (green), however the distribution
633 of species abundance showed a more normal distribution.

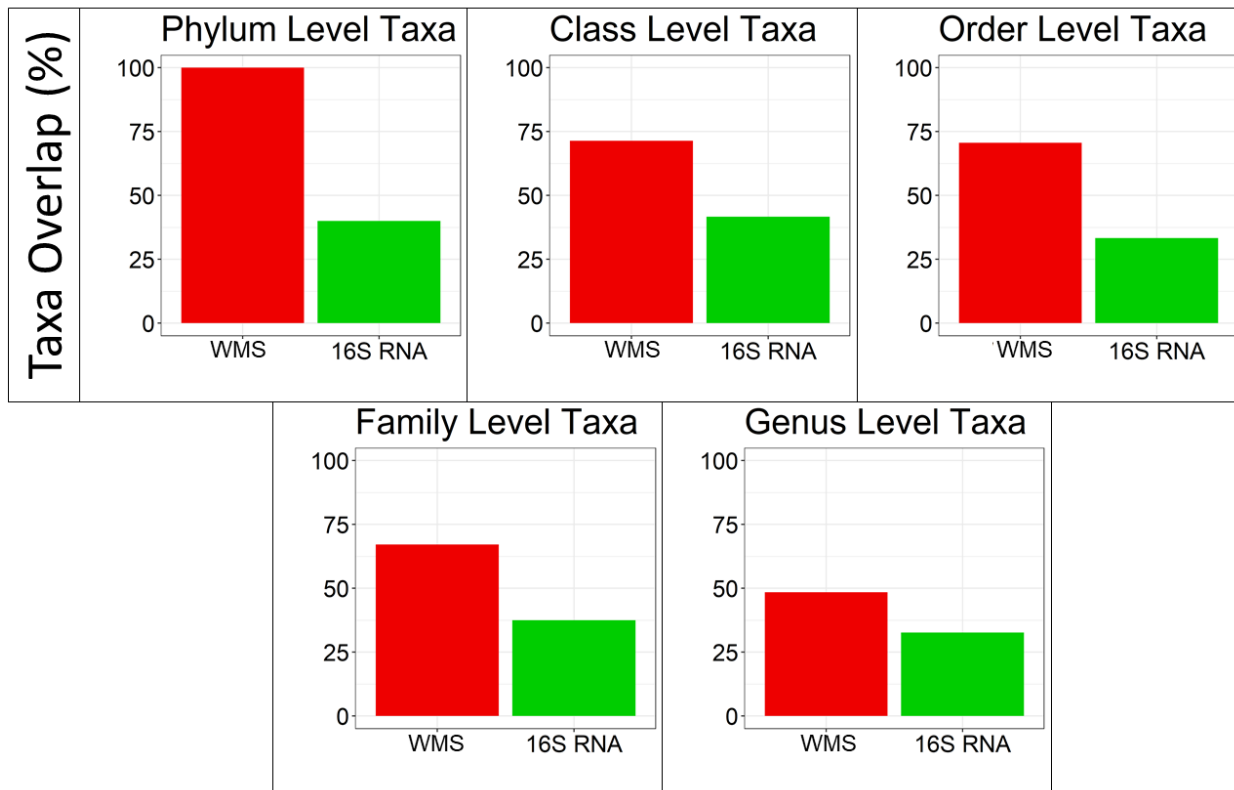
Biegert et al 2020



634

635 **Figure 2. Comparison of top 10 taxa at highest and lowest taxonomic levels for**
636 **WMS and 16sRNA.**

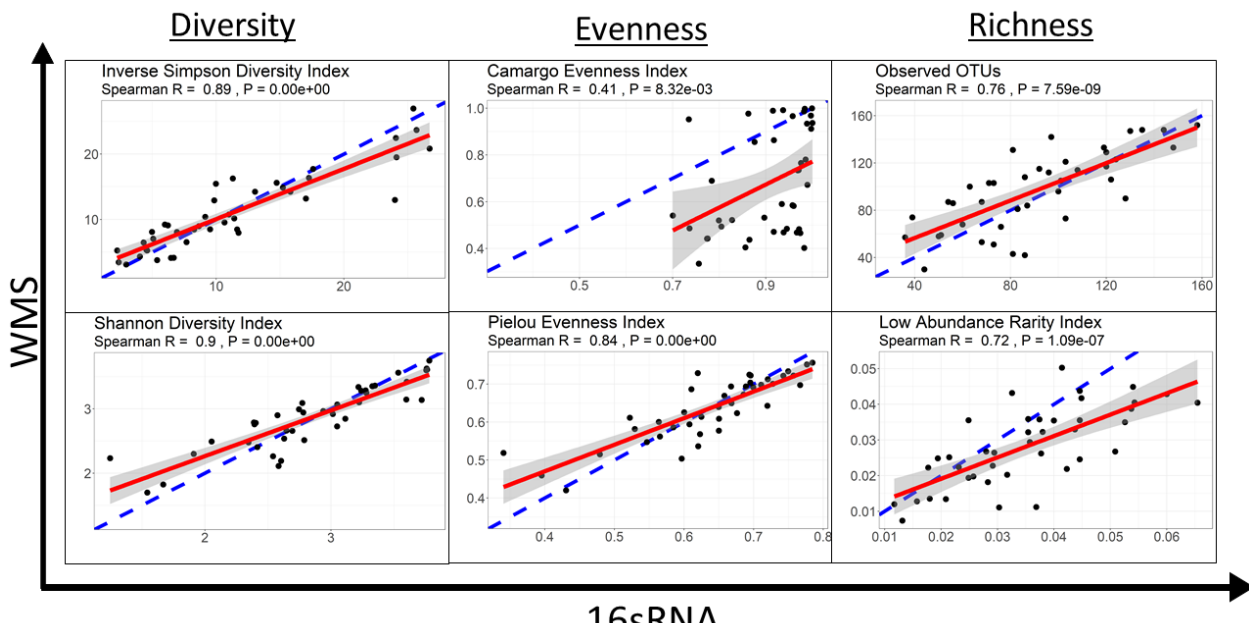
637 The bar plots presented show the top ten most abundant taxa present in the WMS (red),
638 16sRNA (green) as identified at the Phylum and Genus levels of taxa. The two datasets
639 have a greater level of consensus in terms of microbial abundance at higher taxonomic
640 levels (eg. Phylum) than lower levels (eg. Genus).



641

642 **Figure 3. Comparison of number of overlapping taxa at each phylogenetic level**
643 **for WMS and 16S RNA.**

644 The bar plots show the percentage of taxa present in WMS (red), and 16S (green)
645 which overlap in both lists. Across all levels, many of the WMS taxa identified were also
646 identified in the list of 16S taxa.



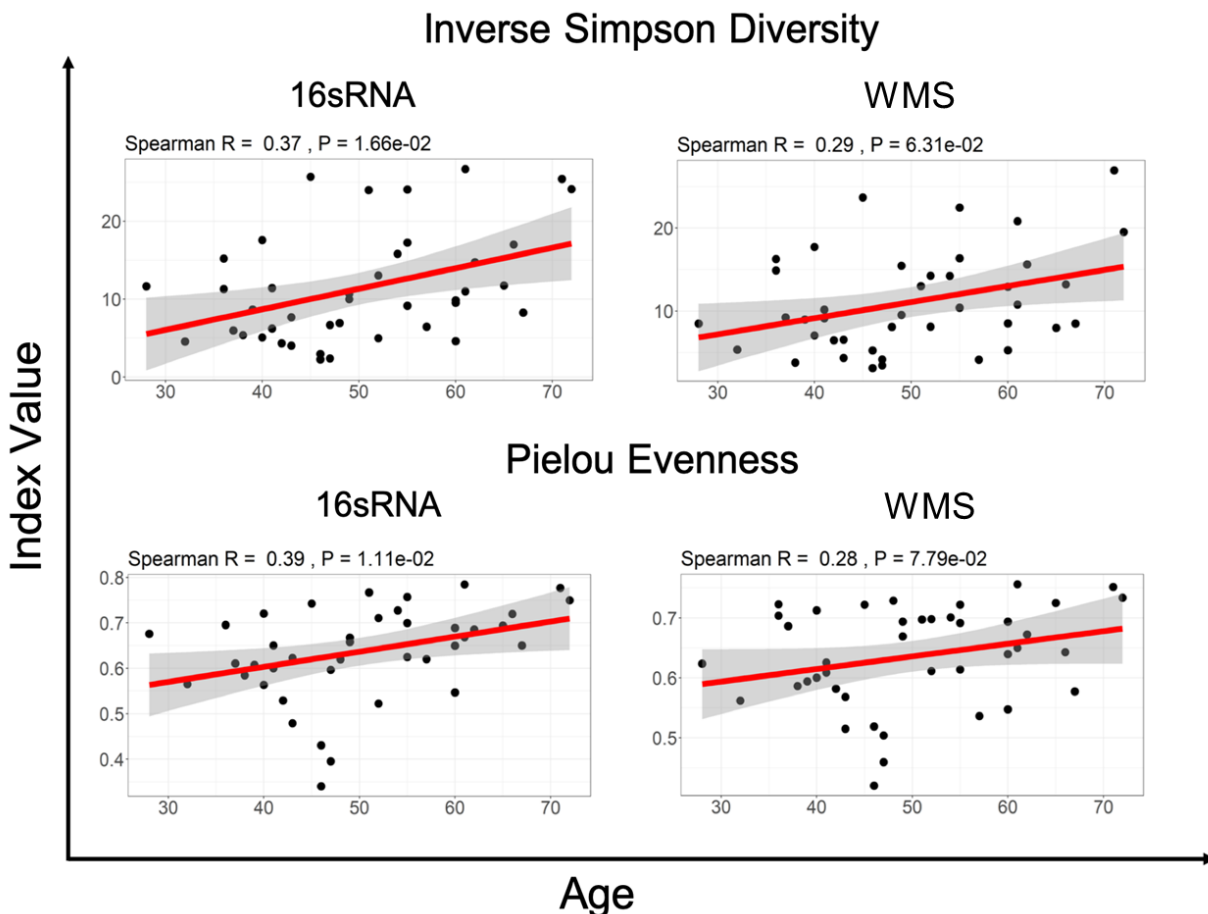
647

16sRNA

648 **Figure 4. Correlation between WMS and 16sRNA in terms of diversity, evenness, and richness.**

649 In this figure, each data point represents a single patient. Consensus between both
650 sequencing methods in terms of alpha diversity is calculated by a Spearman Correlation
651 (R). The slope of the correlation is represented by a red line, while the 95% confidence
652 interval is represented by a grey shaded area. The data derived from 16S sequencing
653 correlates well with the diversity assessment values derived from WMS for diversity and
654 richness. The evenness measures suggest that the sequencing methods differ in terms
655 of the proportionality of individual bacterial taxa.

Biegert et al 2020



657

658 **Figure 5. Correlation between age and Inverse Simpson Diversity and Pielou**

659 **Evenness for 16S vs WMS.**

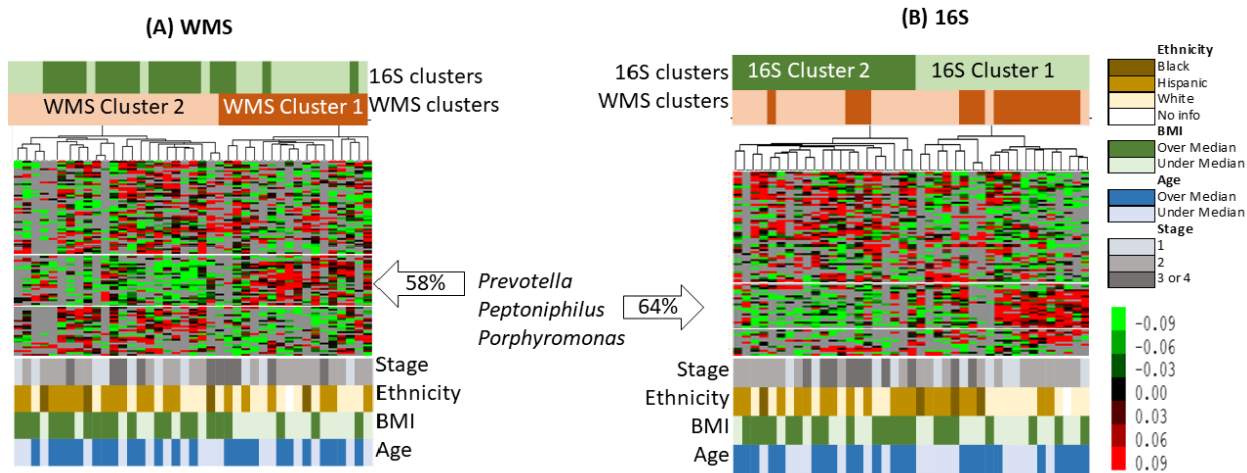
660 The slope of the correlation is shown in red while the 95% confidence interval is indicated

661 by the grey shaded region. Spearman Correlation shows a weak association between

662 age and the Inverse Simpson Diversity Index value as well as the Pielou evenness

663 Index value, for both 16sRNA and WMS data.

Biegert et al 2020



664

665 **Figure 6. Unsupervised hierarchical clustering of samples in terms of putative**
666 **species abundances identified by WMS and by 16S.** To generate these heat maps,
667 only OTUs found in more than 14 samples were considered; 91 OTUs in 16S OTU table
668 and 103 in the WMS OUT table. Overlay between 16S and WMS sample Clusters are
669 shown at the bars above the heat map, while demographic data is presented at the
670 bottom.

671

672 **Supplementary Information**

673 **Supplementary Table 1. Baseline patient demographic information**

674 Patient demographic information was collected prior to initiation of standard treatment
675 and reported here. These demographics were used as patient categories for
676 downstream analysis of microbial diversity, evenness and richness. Ethnicity, History of
677 smoking, Tumor Histology, Node Level, and FIGO Stage were categorical clinical
678 variables while BMI was used as a continuous variable. Age was used both as a

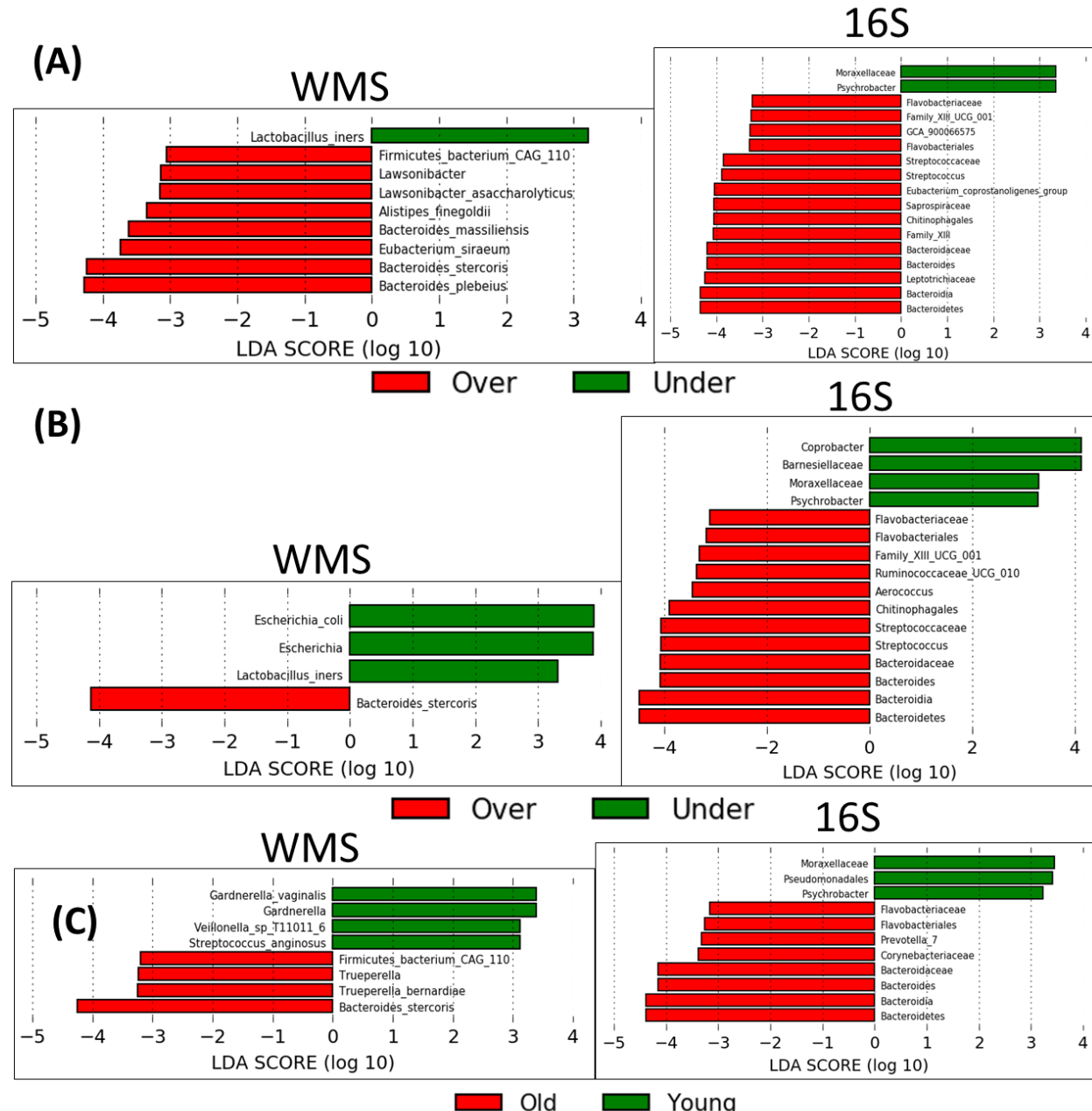
Biegert et al 2020

679 categorical variable (Over vs Under 50 years of Age; Over vs Under Median Age), and
680 as a continuous variable.

Variable	Category	N(%)
Age	Under 50	22(53.66)
	Over 50	19(46.34)
Ethnicity	B	4(9.76)
	H	19(46.34)
	O	1(2.44)
History of smoking	W	17(41.46)
	Yes	17(41.46)
	No	24(58.54)
Histology	Adenocarcinoma	8(19.51)
	Adenosquamous	2(4.88)
	Squamous Carcinoma	31(75.61)
Node Level	Common Iliac	6(14.63)
	External Iliac	15(36.58)
	Internal Iliac	4(9.76)
	Para-Aortic	3(7.32)
	None	13(31.71)
FIGO Stage	IA1	1(2.44)
	IB1	1(2.44)
	IB2	6(14.63)
	IBI	2(4.88)
	IIA	2(4.88)
	IIB	19(46.34)
	IIIB	7(17.07)
	IVA	3(7.32)
Age	Mean \pm SD	Range
	49.98 \pm 10.92	28 – 72
	BMI	28.92 \pm 6.14
BMI		17.5 – 46.7

681

Biegert et al 2020



682

683 **Supplementary Figure 1. LEfSe analysis performed using 3 methods of age**
 684 **classification.**

685 In order to elucidate differences in enriched taxa according to the age clinical variable,
 686 patients were classified using three different metrics: A) Over vs under 50 years of age,

Biegert et al 2020

687 B) Over vs under the median age of all patients, and C) the youngest third of patients
688 (14 individuals) vs the oldest third of patients (14 individuals) in the cohort. WMS and
689 16S datasets were submitted to LEfSe analysis separately, and the resulting bar charts
690 are shown here.

691

Figure 1

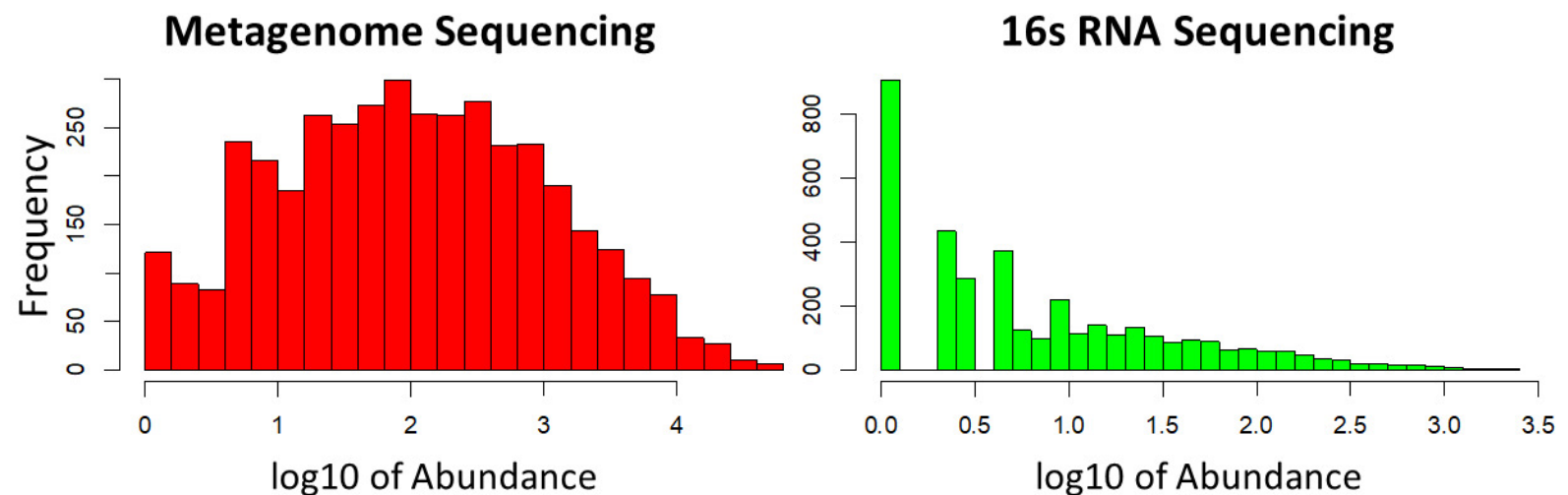


Figure 1. Different distribution of putative taxa species abundance in WMS and in 16S OTU tables. To display differences in abundances in terms of OTU frequencies, OTU counts were log transformed and presented here as histograms. WMS (red) OTU identifiers displayed reduced overall frequency compared to 16S (green), however the distribution of species abundance showed a more normal distribution.

Figure 2

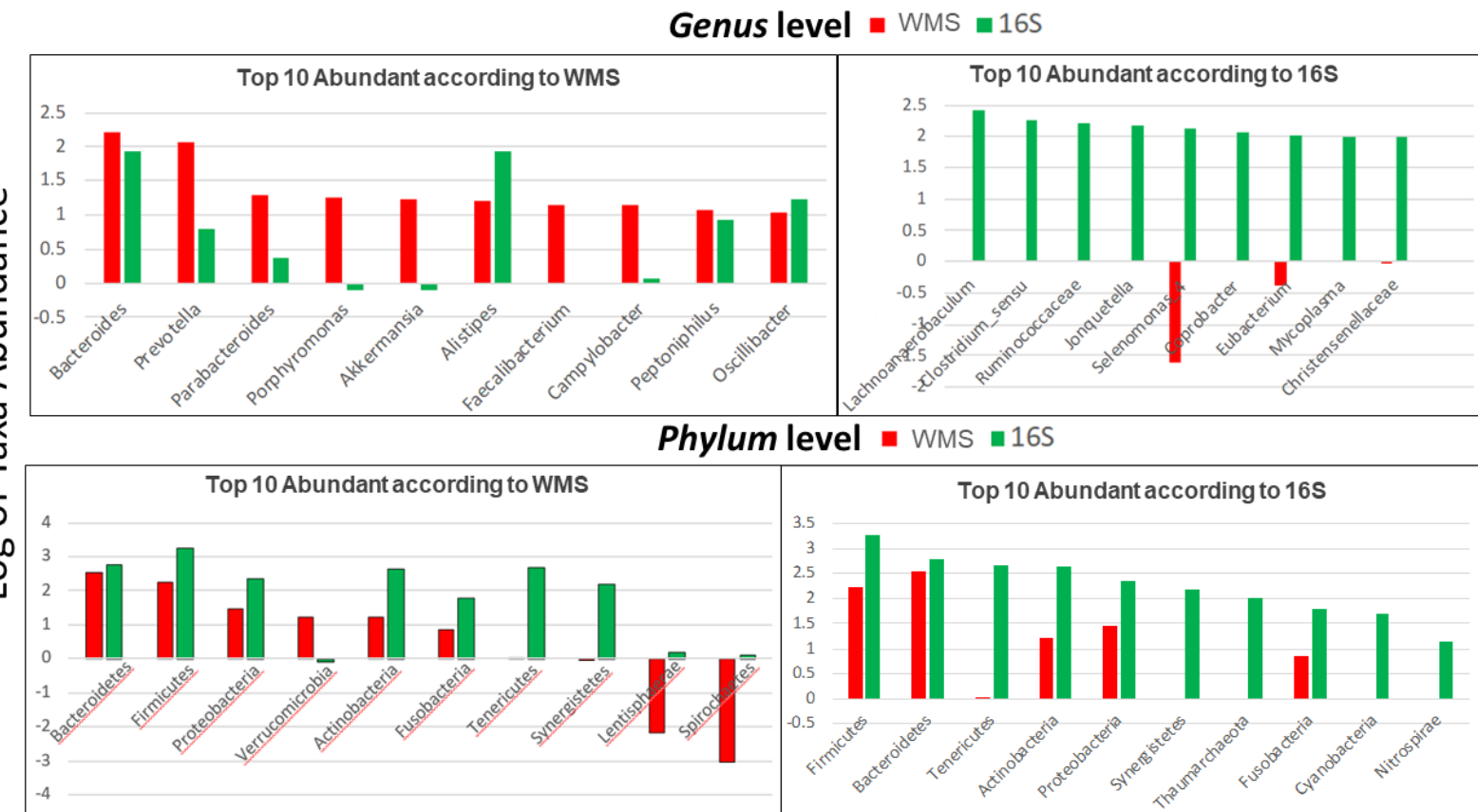


Figure 2. Comparison of top 10 taxa at highest and lowest taxonomic levels for WMS and 16sRNA. The bar plots presented show the top ten most abundant taxa present in the WMS (red), 16sRNA (green) as identified at the Phylum and Genus levels of taxa. The two datasets have a greater level of consensus in terms of microbial abundance at higher taxonomic levels (eg. Phylum) than lower levels (eg. Genus).

Figure 3

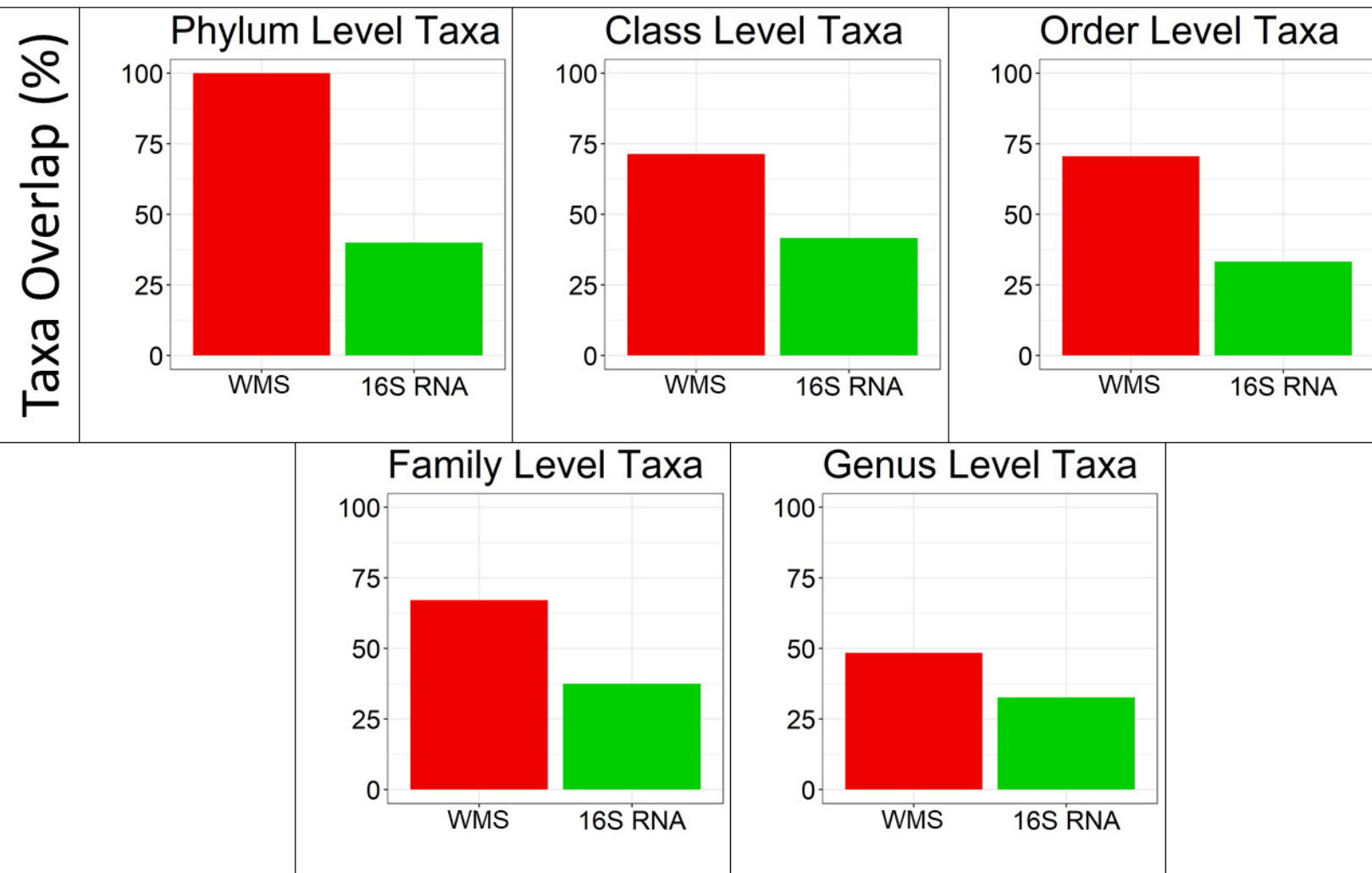


Figure 3. Comparison of number of overlapping taxa at each phylogenetic level for WMS and 16S RNA. The bar plots show the percentage of taxa present in WMS (red), and 16S (green) which overlap in both lists. Across all levels, many of the WMS taxa identified were also identified in the list of 16S taxa.

Figure 4

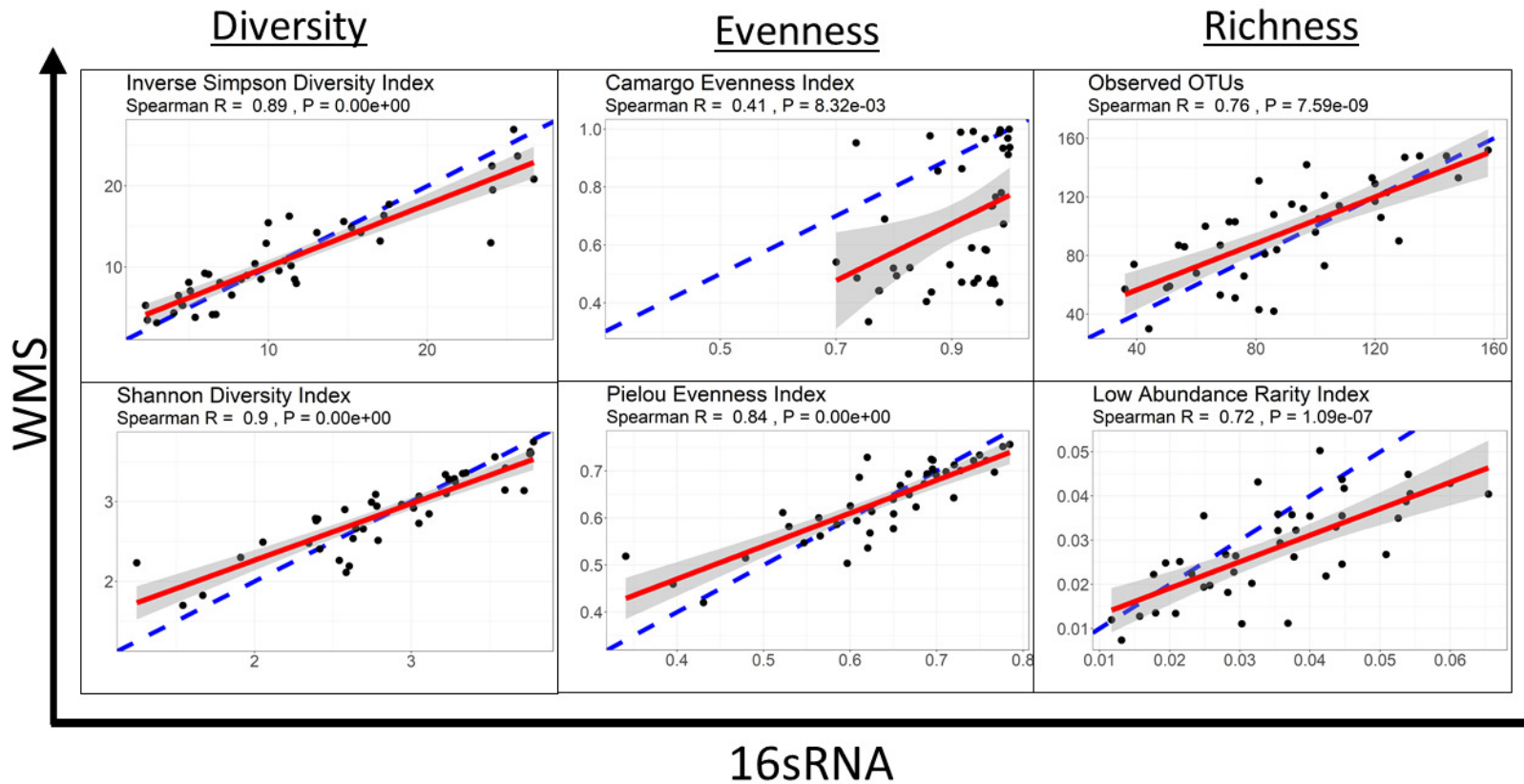


Figure 4. Correlation between WMS and 16sRNA in terms of Diversity, Evenness, and Richness. In this figure, each data point represents a single patient. Consensus between both sequencing methods in terms of alpha diversity is calculated by a Spearman Correlation (R). The slope of the correlation is shown by a red line, while the blue dotted line represents the ideal correlation ($R=1$) and the 95% confidence interval is represented by a grey shaded area. The data derived from 16sRNA sequencing correlates well with the diversity assessment values derived from whole-metagenome sequencing for diversity and richness. The evenness measures suggest that the sequencing methods differ in terms of the proportionality of individual bacterial taxa.

Figure 5

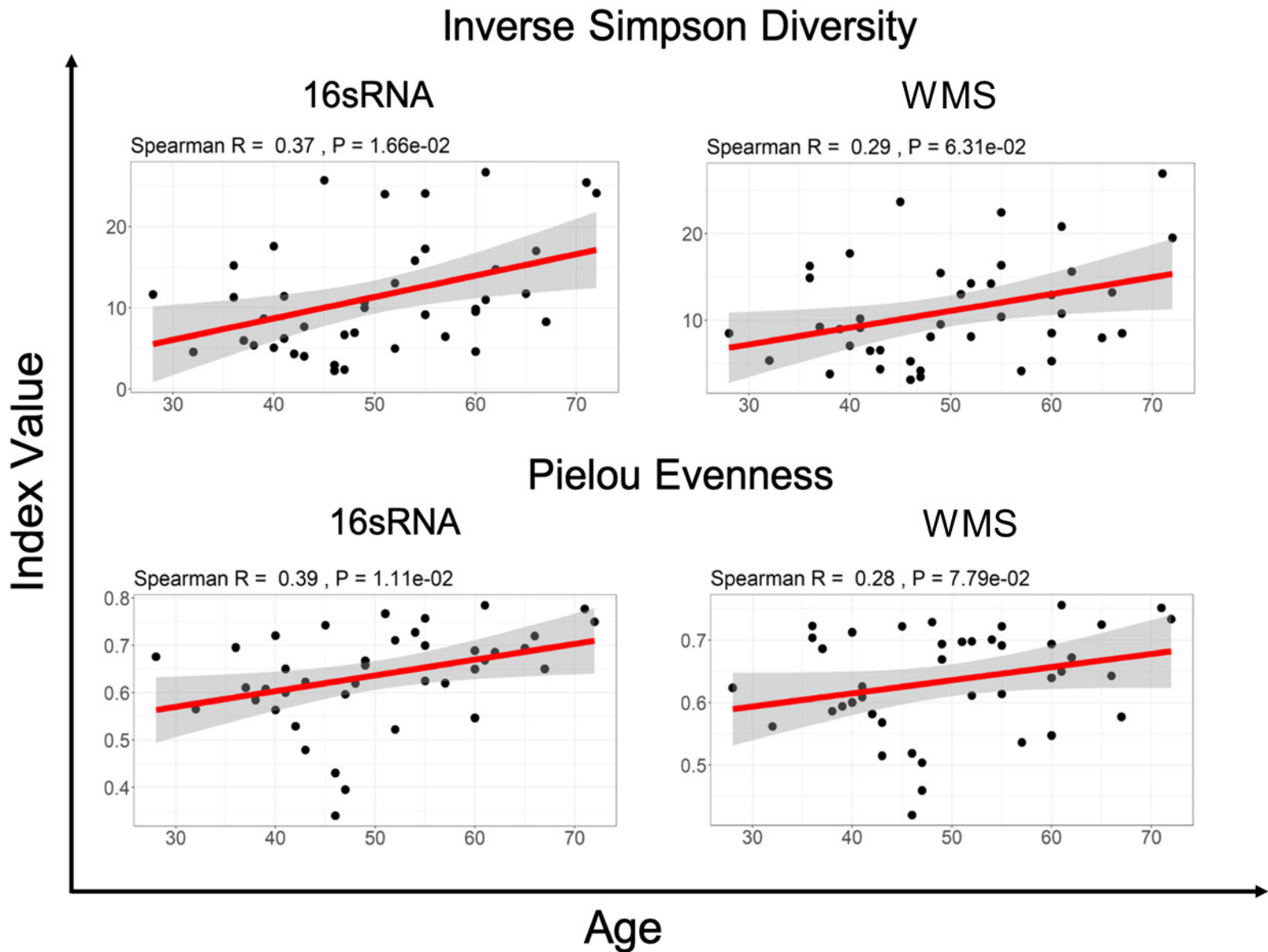


Figure 5. Correlation between age and Inverse Simpson Diversity and Pielou Evenness for 16S rRNA vs WMS. The slope of the correlation is shown in red while the 95% confidence interval is indicated by the grey shaded region. Spearman Correlation shows a weak association between age and the Inverse Simpson Diversity Index value as well as the Pielou evenness Index value, for both 16sRNA and WMS data

Figure 6

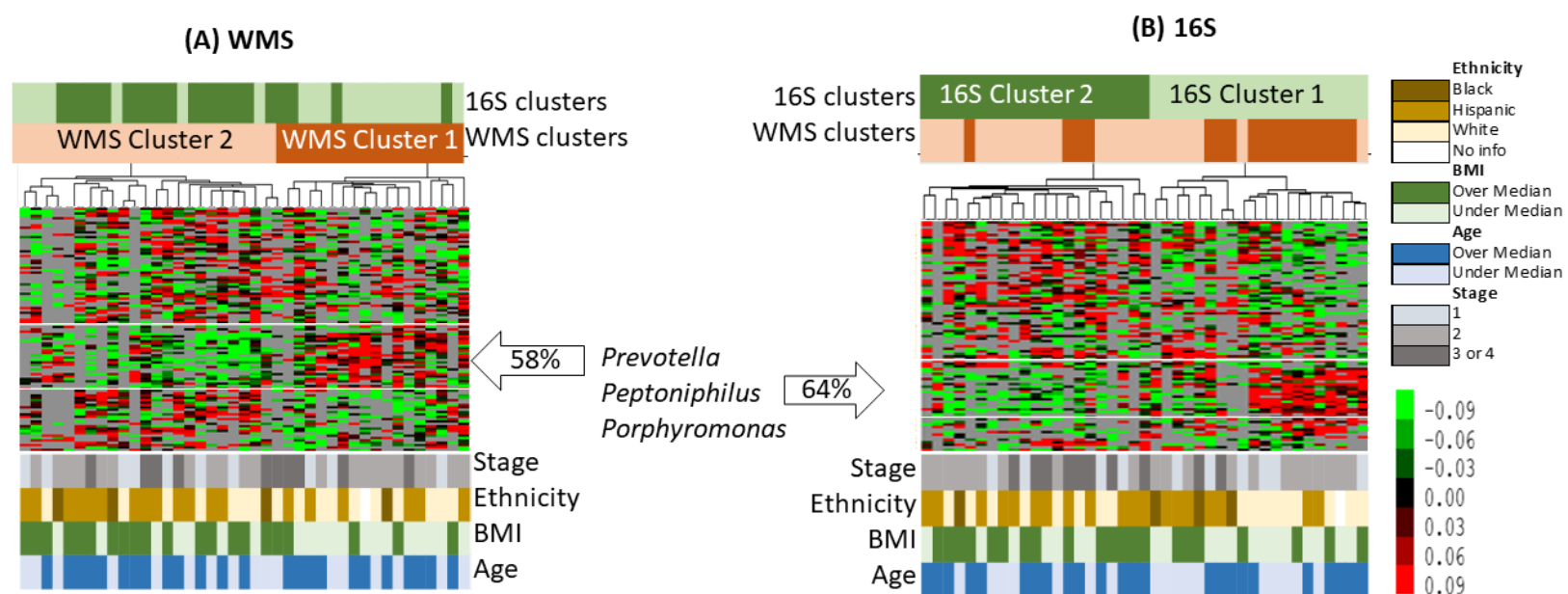


Figure 6. Unsupervised hierarchical clustering of samples in terms of putative species abundances identified by WMS and by 16S. To generate these heat maps, only OTUs found in more than 14 samples were considered; 91 OTUs in 16S OTU table and 103 in the WMS OUT table. Overlay between 16S and WMS sample Clusters are shown at the bars above the heat map, while demographic data is presented at the bottom.

<u>Genus Name</u>	<u>WMS Rank</u>	<u>16S RNA Rank</u>	<u>Spearman R</u>	<u>p Value</u>
Bacteroides	1*	12	0.29	0.0639
Prevotella	2*	70	0.21	ns
Parabacteroides	3*	88	0.09	ns
Porphyromonas	4*	126	-0.1	ns
Akkermansia	5*	129	0.18	ns
Alistipes	6*	13	-0.27	0.0828
Faecalibacterium	7*	-	-	-
Campylobacter	8*	115	0.05	ns
Peptoniphilus	9*	56	0.68	1.14E-06
Oscillibacter	10*	34	0.12	ns
Mycoplasma	58	9*	0.24	ns
Coprobacter	73	7*	0.22	ns
Jonquetella	119	5*	-0.18	ns
Nocardioides	-	1*	-	-
Lachnoanaerobaculum	-	2*	-	-
Clostridium sensu stricto 1	-	3*	-	-
Ruminococcaceae UCG_014	-	4*	-	-
Selenomonas_4	-	6*	-	-
Eubacterium coprostanoligenes group	-	8*	-	-
Christensenellaceae R_7_group	-	10*	-	-

Clinical Variable	Diversity				Evenness				Richness			
	Inverse Simpson		Shannon		Camargo		Pielou		Observed OTUs		LAR	
	WMS	16sRNA	WMS	16sRNA	WMS	16sRNA	WMS	16sRNA	WMS	16sRNA	WMS	16sRNA
Age	0.0631	0.0166	ns	0.0396	0.0077	ns	ns	0.0111	ns	ns	ns	ns
Ethnicity (W,B,H,O)	ns	ns	ns	ns	ns	ns	ns	ns	ns	ns	ns	ns
Smoking History (Y/N)	ns	ns	ns	ns	ns	ns	ns	ns	ns	ns	ns	ns
Histology (Adeno/Squam)	ns	ns	ns	ns	ns	ns	ns	ns	ns	ns	ns	ns
Node level	ns	ns	ns	ns	ns	ns	ns	ns	0.0748	ns	ns	ns
FIGO Stage	ns	ns	ns	ns	ns	ns	ns	ns	ns	ns	ns	ns
BMI	ns	ns	ns	ns	ns	ns	ns	ns	ns	ns	0.0468	ns